International Journal of Research Publication and Reviews

Journal homepage: www.ijrpr.com ISSN 2582-7421

Groundwater Potential in Parts of Bonny Local Government Area, Rivers State, Nigeria

Ebenezer B. Jumbo[1], Etim D. Uko[2], Onengiyeofori A. Davies[3], Amgara O. Tamunokuro[4]

[1,2,3]Department of Physics, Rivers State University, P. M. B. 5080, Port Harcourt, Nigeria

[4]Department of Industrial Safety and Environmental Engineering, Kenule Beeson Saro-Wiwa Polytechnic, Bori, Rivers State University, Nigeria

ABSTRACT

This research involves the analysis of the spatial distribution of groundwater potential within the Bonny Metropolis, in Rivers State, Nigeria. The study area is located between latitudes 4˚28N and longitude 7˚10E. Ten Vertical Electrical Soundings were carried out with an ABEM Terrameter 300 SAS B in order to determine the groundwater potential distribution using Schlumberger configuration. The data acquired was analyzed and interpreted with the aid of IP2Win and surfer 8 software. Topsoil, clay and sandy formations were encountered. Results from the geoelectric sections reveal three to five layers. The resistivity values for the first layer ranges from 1.73Ωm to 863.6Ωm, the second layer ranges from 0.89Ωm to 788.3Ωm, the highest resistivity value was observed in the third layer with resistivity ranging from 0.5 to 1.22×10^{6}Ωm, the fourth layer ranges from 1.84 to 9.203×10^{3}Ωm and the fifth layer ranges from 62.9 to 12.464×10^{3}Ωm with an infinite thickness. The overburden thickness across the area falls between 5m to 100m with maximum thickness range of 75m to100m towards the North-East area. This coincides with the potential water bearing zone. The water level depth distribution of the area varies between 0.2m to 2.6m and the direction of the water flow is towards the central part of the study area while the highest value of the borehole depth distribution was observed at North-Eastern part and North-Western part with a range of 40 to 57m. The results of this work can be used in selecting suitable sites for groundwater resource exploitation in the study area

Keywords: Groundwater Potential, Vertical Electrical Sounding, Aquifer, Bonny, Niger Delta, Nigeria

1. Introduction

Groundwater is one of nature's most essential resources that occurs in pore spaces and fractures in rock and sediment below the surface of the earth (Naghibi et al., 2015; Nmerukini et al., 2018). It plays a significant role in human well-being, ecological balance, and economic growth (Houghton et al., 2001). About 30% of the world's freshwater is concealed and reserved as groundwater, whereas surface water accounts for only 0.3% in the form of lakes, marshes, reservoirs, and rivers (Senanayake et al., 2016). Groundwater has been found to be a more preferred resource due to its less susceptible contamination than surface water (Naghibi et al., 2017). It can be considered as the largest single fresh water source in many parts of the world, especially during prolonged dry periods (Assaf and Saadeh, 2009). The utility of water is continuously growing and causes groundwater resource stress predictably (Vaux, 2011). Consequently, groundwater extraction has become a significant component of water management and planning, particularly in rural regions (Das and Pardeshi, 2018).

The groundwater potential of a region depends on different facts and it varies from place to place according to its change. Variation of the groundwater potential within a short distance and the same geological formation has also been observed (Dar et al., 2010; Nasir et al., 2018; Choudhari et al., 2018; Pradhan et al., 2018). Compared to soft rock aquifer with high yield capacity, hard rock terrain possesses a limited quantity and is mostly concentrated in the weathered zone and fractured zone. In such a situation, depiction of groundwater potential zones (GWPZs) is necessary for the optimal usage of available water resources to meet the needs of the communities. This type of proper identification is possible with knowledge of the lithological variation, topographical status, slope, rainfall pattern, soil texture, geology, hydrogeological, and geophysical aquifer characteristics (Jhariya et al., 2021; Das, 2019; Oh et al., 2011; Mallick et al., 2014).

Water table level is defined as the surface at which pore pressure is equal to atmospheric pressure (Bevan et al., 2005; Mallick, 2019). Water table level indicates hydraulic gradients of any point, hence it can be useful to identify the area with high groundwater potential (Andualem and Demeke, 2019). Evaluation of potentiality plays an essential domain in groundwater resources through effective planning and management, in terms of its occurrences and accumulation (Yadav et al., 2014). Finding and locating the water-bearing/fractures zones, with the provision of electrical resistivity method is considered as the best and most accepted and generalized technique (Zohdy, 1989; Taylor et al., 1992; Ayolabi, 2005; Majumdar and Pal, 2005; Venkateswaran et al., 2014; Urish and Frohlich, 1990; Ebraheem et al., 1997). The current study employed the above VES method for the evaluation of groundwater potential distribution in Bonny Local Government Area, Rivers State, Nigeria.

2. Location, Geology and Hydrogeologic Setting of the Study Area

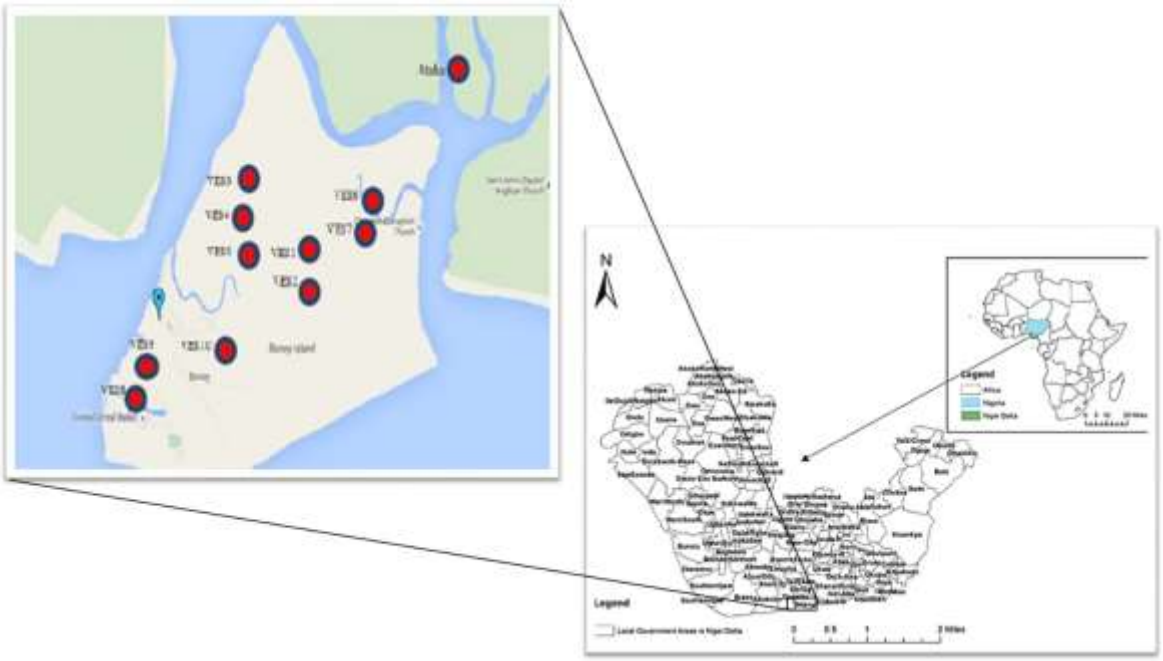

Fig. 1: Map of Bonny Showing the VES Points

The study area Bonny Local Government is an island located in southern part of the Niger Delta, Nigeria (Fig. 1). The physiography conforms to the geomorphic features of the Niger Delta governed by the sediment load, shape and growth of the delta. The Niger Delta lies between latitudes 4°N and 6°N and longitudes 3°E and 9°E (Whiteman, 1982; Adegoke et al., 2017). The coastal sedimentary basin of Nigeria has been the scene of three depositional cycles (Short and Stable, 1967). The first began with a marine incursion in the middle Cretaceous and was terminated by a mild folding phase in Santonian time. The second included the growth of a proto-Niger Delta during the Late Cretaceous and ended in a major Paleocene marine transgression. The third depositional cycle from Eocene to Recent, marked the continuous growth of the main Niger Delta. A new threefold lithostratigraphic subdivision is introduced for the Niger delta subsurface, comprising an upper sandy Benin Formation, an intervening unit of alternating sandstone and shale named the Agbada Formation, and a lower shaly kata Formation.

These three units extend across the whole delta and each range in age from early Tertiary to Recent. They are related to the present outcrops and environments of deposition. A separate member of the Benin Formation is recognized in the Port Harcourt area. It is Miocene-Recent in age with a minimum thickness of more than 6,000ft (1829m) and made up of continental sands and sandstones (> 90%) with few shale intercalations (Horsfall et al., 2017). Subsurface structures are described as resulting from movement under the influence of gravity and their distribution is related to growth stages of the delta (Ochoma et al., 2020). Rollover anticlines in front of growth faults form the main objectives of oil exploration, the hydrocarbons being found in sandstone reservoirs of the Agbada Formation.

The Benin Formation (coastal plain sands) forms the major aquifer in the study area and is exploited for groundwater supply. Although a depth of about 7m is most exploited, about 400m depth has been exploited for water supply in Bonny Local Government Area drilled by NLNG but contains iron and is treated for iron before use by the public. It consists essentially of massive and highly porous sands and gravels with few clay intercalations.

The climate of the study area is tropical and dominated by two main seasons: the dry and rainy seasons. Average mean annual rainfall is over 2400 mm and according to hydro-geological studies over 40% of this infiltrate and recharge groundwater (Amadi et al., 2012). The soil profile is remarkably uniform throughout the area. Approximately, the whole areas consist of deeply weathered and intensely leached soil. The heavy rainfall coupled with the drainage nature of the sub soil is conducive for the high infiltration of rainwater.

The proximity of Nigeria to the equator is responsible for the general high temperature. A mean annual temperature of 270C is recorded in part of the Niger Delta Region. Minimum temperatures in the coastal states are highest in February, March and April and lowest in January and August. Relative humidity near the coast is about 80% to 100% at dawn and 70 to 80% in early afternoon at maximum temperature (Amadi et al., 2012).

The vegetation cover is thick mangrove in a very swampy environment implying significant evapo-transpiration effect. Run-off is limited following the thick vegetation; hence ground water recharge and storage is plentiful in this area. However, the water table is deep (>3m), hence chances of groundwater ex-filtration and evaporation is low. The vegetation is typically tropical rain forest.

3. Materials and Methods

The apparent resistivity (ρ_a) obtained from earth measurements does not vividly represent the true electrical resistivity of the subsurface and may not directly be related to the real value of electrical resistivity in a heterogeneous earth. In reality, its value may be larger or smaller than the actual resistivity, or in rare cases, it may be identical with one of the true resistivity values in a heterogeneous earth (Tipler and Kyker, 1982). Therefore, to obtain the true resistivity of any point in the ground, the apparent resistivity value obtained which describes $\left(\frac{\Delta V}{I}\right)$ measured is multiplied with the appropriate geometrical factor K. In a Schlumberger sounding spread (Fig. 2), the voltage electrodes are usually kept small and fixed while only the C_1C_2 spacing is changed. By convention A, B, M and N in the formula below is equal to C_1, C_2, P_1 and P_2 respectively.

The apparent resistivity, ρ_a, is mathematically, defined as;

$$\rho_a = \frac{(AB)^2-(MN)^2}{MN}\frac{\Delta V}{I} \qquad (1)$$

The geometric factor, K, is mathematically, defined as;

$$K = \frac{(AB)^2-(MN)^2}{MN} \qquad (2)$$

Therefore,

$$\rho_a = K\frac{\Delta V}{I} \qquad (3)$$

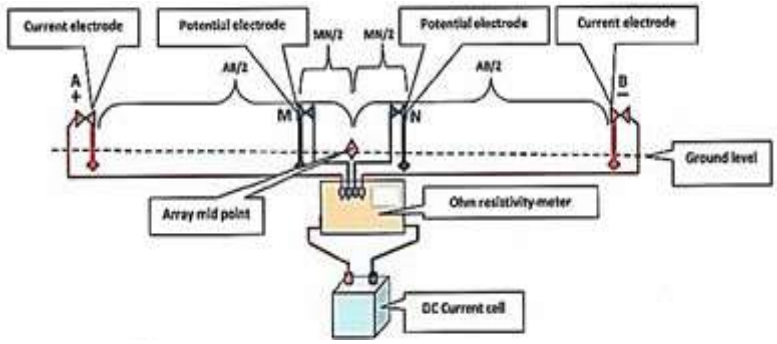

Fig. 2: Schematic Diagram of Schlumberger Array

The basic resistivity Equipment used in the study is an ABEM Terrameter SAS 300 B, a 12 volts battery, four stainless steel electrodes, calibrate tapes, four reels of cables, a hammer and Global Positioning System (GPS). The ABEM Terrameter SAS 300 B is powered internally by a 12 volts battery which supplies the external power source by means of a cable, inbuilt in the instrument. This transmits the power source to the ground through the electrons by means of reams of cables. The method used in this research is the Schlumberger Array and a total of 10 VES station points were taken in different communities in Bonny Local Government Area with minimum and maximum electrode spread length of 300m and 500m respectively. The procedure involved in measuring VES is, first to confirm the functionality of the instrument ABEM Terrameter 300B and battery voltage, then the current electrodes C_1 & C_2 are connected to the instrument and the potential electrodes P_1 & P_2 are also connected to the instrument as indicated on the instrument. The two electrodes C_1 and C_2, on the opposite side of the VES station point, were marked and noted and the driven to the ground with the aid of a sledgehammer for better contact to the ground. Similarly, the two other electrodes P_1 & P_2 were equally measured and driven to the ground for proper contact. The current and potential electrodes were both placed so as to maintain a straight line. The potential electrodes P_1 & P_2 were placed with varying spacing which was not more than one fifth of the current electrodes, C_1 & C_2, spacing. The current electrode spacing was placed at progressively large distances. The separation of the potential electrodes was increased in accordance with the corresponding increase in distance between the current electrodes. Measurement continued and the potential electrodes separation increased again as necessary until the Vertical Electrical Sounding (VES) was complete. At every corresponding interval between the current electrode and the potential electrode, the resistivity value was obtained.

The acquired data was interpreted using IP2Win software. The result from the software were then analyzed based on the number of layers, the resistivity, the depth of aquifer and the thickness observed. The result was then compared to the type of resistivity sounding curve observed in the study area in order to delineate areas of low and high resistivity values in order to demarcate areas of thick aquifer and ground water potential. The process was made possible to estimate the resistivities of the various geo-electric layers, while sulfer8 software was used to generate Iso-pach and iso-resistivity of the various locations which gives details of the overburden thickness and resistivity of the various subsurface formation.

Results and Discussion

4.1 Isopach

Fig. 3 presents the Isopach plot of the Study. It displays the lateral/horizontal dissimilarity of how thick the overburdens are. The overburden thickness range from 2m-100m (Fig. 3).

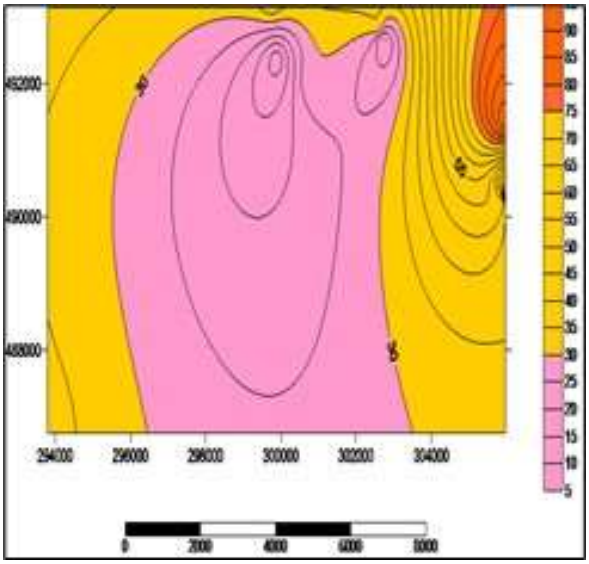

Fig. 1: Isopach May of the Study Area

The study revealed that that the overburden thickness is low at that central part of the study area with thick of 5m to 25m. The Map also revealed medium thickness range of 30m to 70m at the East-Western part of the area. Towards the North-East area, the overburden thickness is large with maximum thickness range of 75m to 100m. This coincides with the potential water bearing zone in a complex basement terrain. Hence, this part is termed the water potential zone.

4.2 Iso-Resistivity at AB/2=10m

The iso-resistivity map presents the sideways deviation of the resistivity over a certain layer at a particular depth in the survey area (Fig. 4).

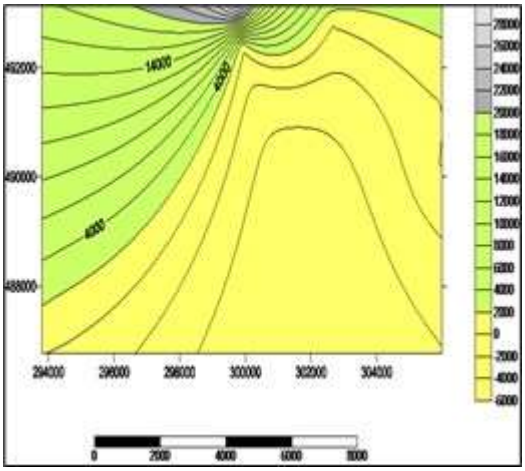

Fig. 2: Iso-resistivity at AB/2=10m

The map represents how apparent resistivity is dispensing in the area when plotted with the current electrode values. Figure 4 represent the iso-resistivity at AB/2=10m. The map reveals the resistivity varies between -250 to 12,500Ωm. the map revealed a low resistivity value at the Centre between -250 to 500Ωm. the low value of the resistivity depicts the top soil formation. Area with medium resistivity value range of 500Ωm to 3,500Ωm fall between the West, and North-East while area of high resistivity depicted to be water potential zone falls on the North-west part with resistivity value range of 4,500Ωm to 1,200Ωm.

4.3 Iso-Resistivity at AB/2=30m

The iso-resistivity shown in Fig. 5 indicate that the resistivity of the formation ranges from -6,000Ωm to 32,000Ωm.

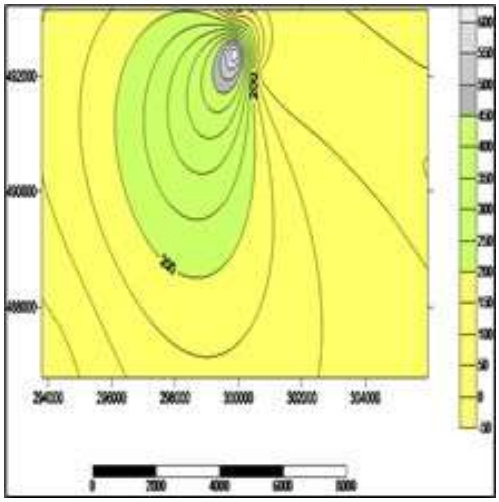

Fig. 3: Iso-Resistivity at AB/2=30m

Area of low resistivity lies in the central part with resistivity value of -6,000Ωm to 0Ωm. the resistivity values shows that this part is not a potential zone. Area with medium resistivity value fall within the western part of the area has apparent resistivity range of 2,000Ωm to 1,800Ωm, while region of high apparent resistivity assumed to zone of coarse sand and potential zone has resistivity value of 20,000Ωm to 32,000Ωm.

4.4 Iso-Resistivity at AB/2=60m

Fig. 6 show the iso-resistivity map at AB/2 = 60m.

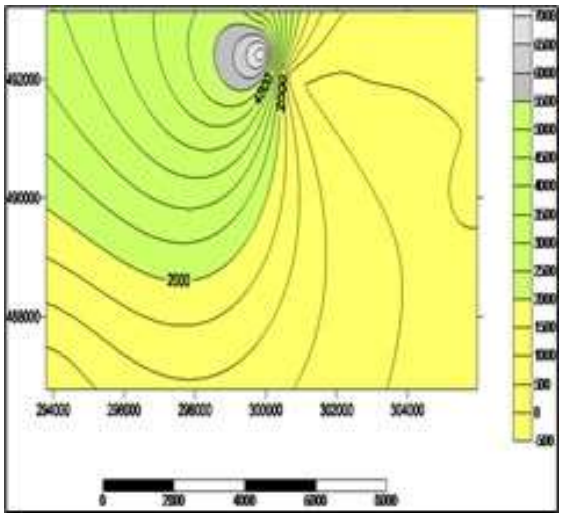

Fig. 4: Iso-Resistivity at AB/60m

From the Map, it is shown that the resistivity revealed the composition of topsoil, sandy-Soil to Clay formation lies along North-East , South-East and part of the West of the Study area, the apparent resistivity lies between -50 t0 650Ωm with the highest potential area at the North with a range of 450 to 650Ωm.

4.5 Iso-Resistivity at AB/2=100m

Fig. 7 indicate iso-resistivity at AB/2=100m. it is seen here that the apparent resistivity begins at -1,000Ωm – 17,000Ωm. Zone of high potential fall between 1,100Ωm to 17,000Ωm along the northern part of the area.

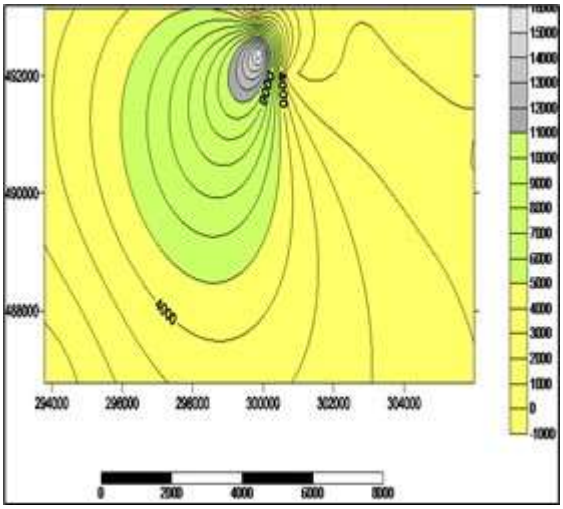

Fig. 5: Iso-Resistivity at AB/2=100m

4.6 Iso-Resistivity at AB/2=150m

Fig. 8 represent the iso-Resistivity at 150m.

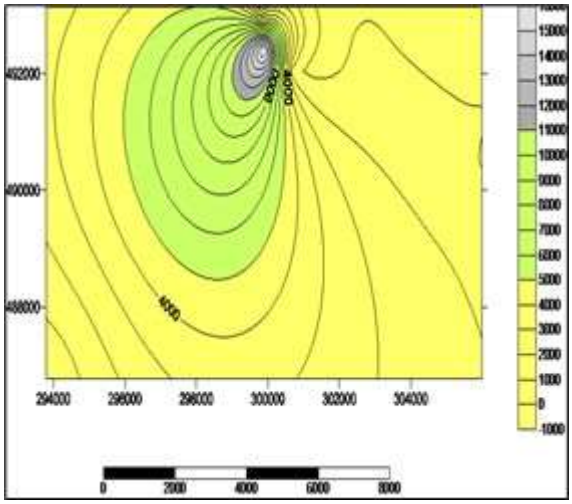

Fig. 6: Iso-Resistivity at AB/2=150m

The Map revealed that the apparent resistivity value ranges from -500 to 1,500Ωm. The zone of high potential lies between 5,500 to 7,500Ωm which is in the Northern part of the study area. Generally, the iso–Resistivity the at AB/100m has the highest apparent value indicating that it the highest water bearing zone

4.7 Water Level Distribution and Borehole Depth Maps

The subsurface maps of water level distribution and borehole depths of the study area were generated and presented as Fig. 9a and 9b which depict the results of the water level distribution and borehole depths of the aquifer encountered. The water level distribution varies from 0.2m to 2.6m. The area colour coded red is observed to be the steepest in the central part of the study area, while the area colour coded with green indicates area that is the shallowest. The other area colour coded blue indicates area that has intermediate water level values. The direction of the water flow is indicated by the arrow pointing towards the steepest areas. From the map it can be suggested that the direction of underground water in the study area is towards the central parts of the study area (Fig. 9a). Fig. 9b shows how borehole depth is spread within the study area. The highest value of the depth distribution is seen at North-Eastern parts and North-Western part with a range of 40 to 57m. The area coded with yellow indicates areas that has the lowest borehole depths (40-46m). The areas colour coded with colour green are areas of intermediate borehole depths (47 – 51m) while the areas colour coded with ash indicates the areas that has the highest borehole depths.

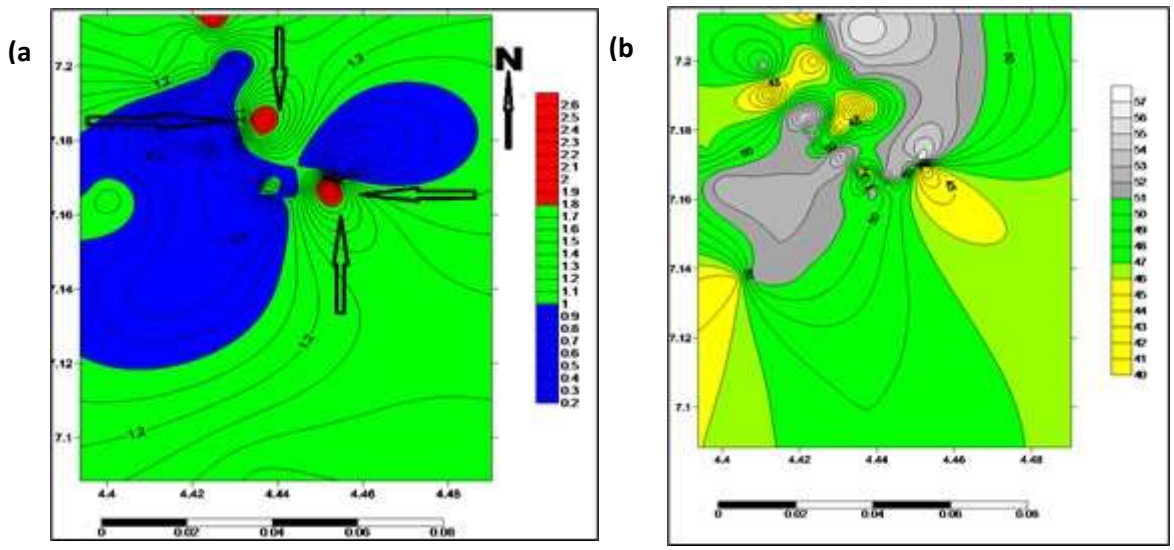

Fig. 1: (a) Water Level Depth (b) Borehole Depth

5. Conclusion

The passage of current into the ground by adopting VES techniques in the area has immensely helped in knowing the overburden depths and potential zones of the study area. Topsoil, clay and sandy formations were encountered and the result from the Geoelectric sections reveals three to five layers. The resistivity values for the first layer ranges from 1.73Ωm to 863.6 Ωm, the second layer ranges from 0.89 Ωm to 788.3 Ωm, the highest resistivity value was observed in the third layer with resistivity ranging from 0.5 to 1.22×10^{6}Ωm, the fourth layer ranges from 1.84 to 9.203×10^{3}Ωm, the fifth layer ranges from 62.9 to 12.464×10^{3}Ωm with an infinite thickness. The overburden thickness across the area falls between 5m to 100m. Medium thickness range of 30m to 70m at the East-Western part of the area. Towards the North-East area, the overburden thickness is large with maximum thickness range of 75m to 100m. This coincides with the potential water bearing zone. The water level depth distribution of the area varies between 0.2m to 2.6m and the direction of the water flow is towards the central part of the study area while the highest value of the borehole depth distribution was observed at North-Eastern part and North-Western part with a range of 40 to 57m.

References

Adegoke, O. S., Oyebamiji, A. S., Edet, J. J., Osterloff, P. L., Ulu, O.K. (2017). Cenozoic Foraminifera and Calcareous Nannofossil Biostratigraphy of the Niger Delta. Elsevier, Cathleen Sether, United States.

Amadi, A. N. ,Olasehinde, P. I., Yisa, J., Okosun, E. A.,Nwankwoala, H. O., Alkali, Y. B. (2012). Geostatistical assessment of Groundwater Quality from Coastal Aquifers of Eastern Niger Delta, Nigeria. International Journal of Geosciences, 2, 51-59.

Andualem, T. G., Demeke G. G. (2019). Groundwater Potential Assessment Using GIS and RemoteSensing: A Case Study of GunaTana Landscape, Upper Blue Nile Basin, Ethiopia. Journal of Hydrology, 24.

Assaf, H., Saadeh, M. (2009).Geostatistical Assessment of Groundwater Nitrate Contamination with Reflection on DRASTIC Vulnerability Assessment: The Case of the Upper Litani Basin, Lebanon. Water Resources Management, 23, 775–796.

Ayolabi, E. A. (2005). Geoelectric Evaluation of Groundwater Potential: A Case Study of Alagbaka Primary School, Akure Southwest Nigeria. Journal of the Geological Society of India, 66, 491-495.

Bevan, M. J., Endres, A. L., Rudolph, D. L., Parkin, G. (2005). A Field Scale Study of Pumping-Induced Drainage and Recovery in an Unconfined Aquifer. Journal of Hydrology, 31552-70.

Choudhari, P. P., Nigam, G. K., Singh, S. K., Thakur, S. (2018). Morphometric Based Prioritization of Watershed for Groundwater Potential of Mula River Basin, Maharashtra, India. Geology, Ecology, and Landscapes, 2, 256–267.

Dar, I. A., Sankar, K., Dar, M. A. (2010). Remote SensingTechnology and Geographic Information System Modeling: An Integrated Approach Towards the Mapping of Groundwater Potential Zones in Hardrock Terrain, Mamundiyar Basin. Journal of Hydrology, 394, 285–295.

Das, S. (2019). Comparison among Influencing Factor, Frequency Ratio, and Analytical Hierarchy Process Techniques for Groundwater Potential Zonation in Vaitarna Basin, Maharashtra, India. Groundwater for Sustainable Development, 8, 617-629.

Das, S., Pardeshi, S. D. (2018). Morphometric Analysis of Vaitarna and Ulhas River Basins, Maharashtra, India: Using Geospatial Techniques. Applied Water Science, 8.

Ebraheem, A. A. M., Senosy, M. M., Dahab, K. A. (1997). Geoelectrical and Hydrogeochemical Studies for Delineating Groundwater Contamination due to Salt-Water Intrusion in the Northern part of the Nile Delta, Egypt. Ground Water, 35, 216-222.

Houghton, J. T., Ding, Y., Griggs, D. J., Noguer, M., Vander Linden, P. J., Dai, X., Maskell, K., Johnson, C. A. (2001). Climate Change: The Scientific Basis. Cambridge University Press: Cambridge, UK.

Horsfall, O. I., Uko, E. D., Tamunobereton-ari, I., OmuboPepple, V. B. (2017). Rock-Physics and Seismic-Inversion Based Reservoir Characterization of AKOSFIELD, Coastal Swamp Depobelt, Niger Delta. Applied Geology and Geophysics, 5, 59-67.

Jhariya, D. P., Khan, R., Mondal, K. C., Kumar, T., Indhulekha, K., Singh, V. K. (2021). Assessment of Groundwater Potential Zone Using GIS-Based Multi-Influencing Factor (MIF), Multi-Criteria Decision Analysis (MCDA) and Electrical Resistivity Survey Techniques in Raipur City, Chhattisgarh, India. Journal of Water Supply: Research and Technology-Aqua, 70, 375–400.

Majumdar, R. K., Pal, S. K. (2005). Geoelectric and Borehole Lithology Studies for Groundwater Investigation in Alluvial Aquifer of Munger District, Bihar. Journal of the Geological Society of India, 66, 463–474.

Mallick, J.,Al-Wadi, H., Rahman, A., Ahmed, M. (2014). Landscape Dynamic Characteristics Using Satellite Data for a Mountainous Watershed of Abha, Kingdom of Saudi Arabia. Environmental Earth Sciences, 72, 4973-4984.

Mallick, J., Khan, R.A., Ahmed, M., Alqadhi, S. D., Alsubih, M., Falqi, I., Hasan, M. A. (2019). Modeling Groundwater Potential Zone in a Semi-Arid Region of Aseer Using Fuzzy-AHP and Geoinformation Techniques. Water, 11, 2656.

Naghibi, S. A., Moghaddam, D. D., Kalantar, B., Pradhan, B., Kisi, O. (2017). A comparative Assessment of GIS-Based Data Mining Models and a Novel Ensemble Model in Groundwater Well Potential Mapping. Journal of Hydrology, 548, 471–483.

Naghibi, S. A., Pourghasemi, H. R., Pourtaghi, Z. S., Rezaei, A. (2015). Groundwater Qanat Potential Mapping Using Frequency Ratio and Shannon's Entropy Models in the Moghan Watershed, Iran. Earth Science Informatics, 8, 171-186.

Nasir, M. J., Khan, S., Zahid, H., Khan, A. (2018). Delineation of Groundwater Potential Zones Using GIS and Multi-Influence Factor(MIF) Techniques: A Study of District Swat, Khyber Pakhtunkhwa, Pakistan. Environmental Earth Sciences, 77, 367.

Nmerukini I., Uko, E. D., Tamunobereton-ari, I. (2018). Groundwater Level Distribution and Evaluation of Physicochemical Characteristics in North-Eastern Bayelsa State, Nigeria. International Journal of Scientific and Engineering Research, 9.

Ochoma, U., Uko, E. D., Ayanninuola, O. S. (2020). Subsurface Structures of Onshore Fuba Field, Niger Delta, Nigeria. International Journal of Scientific Researchin in Physics and Applied Sciences, 8, Pp. 38-44.

Oh, H. J., Kim, Y. S., Choi, J. K., Park, E., Lee, S. (2011). GIS Mapping of Regional Probabilistic Groundwater Potential in the Area of Pohang City, Korea. Journal of Hydrology, 399, 158-172.

Pradhan, R. K., Srivastava, P. K., Maurya, S., Singh, S. K. Patel, D. P., 2018. Integrated Framework for Soil and Water Conservation in Kosi River Basin Through Soil Hydraulic Parameters, Morphometric Analysis and Earth Observation Dataset. Geocarto International, 35, 1–20.

Senanayake, I. P., Dissanayake, D. M. D. O. K., Mayadunna, B. B., Weerasekera, W. L. (2016). An Approach to Delineate Groundwater Recharge Potential Sites in Ambalantota, Sri Lanka Using GIS Techniques. Geoscience Frontiers, 7, 115-124.

Short, K. C., Stable, A. J. (1967). Outline of Geology of Niger Delta. Bulletin of America Association of Petroleum Geologists, 51, 761-779.

Taylor, K., Widmer, M. Chesley, M. (1992). Use of Transient Electromagneticto Define Local Hydrogeology in an Arid Alluvial Environment. Geophysics, 57, 343–352.

Tipler, P. A., Kyker, G. C. (1982). Study Guide to Accompany Physics, Second Edition. Worth Publishers, New York.

Urish, D. W., Frohlich, R. K. (1990). Surface Electrical Resistivity in Coastal Groundwater Exploration. Geoexploration, 26, 267–289.

Vaux, H. (2011). Groundwater UnderStress: The Importance of Management. Environmental Earth Sciences, 62, 19–23.

Venkateswaran, S., Prabhu, M. V., Karuppannan, S. (2014). Delineation of Groundwater potential zones using geophysical and GIS techniques in the Sarabanga Sub-Basin, Cauvery River, Tamil Nadu, India. International Journal of Current Research and Academics Review, 2, 58–75.

Whiteman, A. (1982). Nigeria: Its Petroleum Ecology Resources and Potential.Graham and Trotman, London.

Yadav, S. K., Singh, S. K., Gupta, M., Srivastava, P. K. (2014). Morphometric Analysis of Upper Tons Basin from Northern Foreland of Peninsular India Using CARTOSAT Satellite and GIS. Geocarto International, 29, 895–914.

Zohdy, A. A. R. (1989). A new Method for Automatic Interpretation of Schlumberger and Wenner Sounding Curves. Geophysics, 54 (2), 245–253